Central Representation of Dynamics When Manipulating Handheld Objects

Theodore E. Milner, David W. Franklin, Hiroshi Imamizu and Mitsuo Kawato

J Neurophysiol 95:893-901, 2006. First published Oct 26, 2005; doi:10.1152/jn.00198.2005

J Neurophysiol 95: 893–901, 2006.
First published October 26, 2005; doi:10.1152/jn.00198.2005.

Central Representation of Dynamics When Manipulating Handheld Objects

Theodore E. Milner,[1,2] David W. Franklin,[1,2] Hiroshi Imamizu,[1] and Mitsuo Kawato[1]
[1]*Computational Neuroscience Laboratories, ATR, Kyoto, Japan; and* [2]*School of Kinesiology, Simon Fraser University, Burnaby, Canada*

Submitted 24 February 2005; accepted in final form 21 October 2005

Milner, Theodore E., David W. Franklin, Hiroshi Imamizu, and Mitsuo Kawato. Central representation of dynamics when manipulating handheld objects. *J Neurophysiol* 95: 893–901, 2006. First published October 26, 2005; doi:10.1152/jn.00198.2005. To explore the neural mechanisms related to representation of the manipulation dynamics of objects, we performed whole-brain fMRI while subjects balanced an object in stable and highly unstable states and while they balanced a rigid object and a flexible object in the same unstable state, in all cases without vision. In this way, we varied the extent to which an internal model of the manipulation dynamics was required in the moment-to-moment control of the object's orientation. We hypothesized that activity in primary motor cortex would reflect the amount of muscle activation under each condition. In contrast, we hypothesized that cerebellar activity would be more strongly related to the stability and complexity of the manipulation dynamics because the cerebellum has been implicated in internal model-based control. As hypothesized, the dynamics-related activation of the cerebellum was quite different from that of the primary motor cortex. Changes in cerebellar activity were much greater than would have been predicted from differences in muscle activation when the stability and complexity of the manipulation dynamics were contrasted. On the other hand, the activity of the primary motor cortex more closely resembled the mean motor output necessary to execute the task. We also discovered a small region near the anterior edge of the ipsilateral (right) inferior parietal lobule where activity was modulated with the complexity of the manipulation dynamics. We suggest that this is related to imagining the location and motion of an object with complex manipulation dynamics.

INTRODUCTION

The stability of dynamic interactions between humans and common implements that we employ as tools and instruments can vary widely. Our ability to use implements effectively requires that we be able to adapt to differences in dynamics. With experience we can quickly change patterns of muscle activation to adjust to differences in mass, moment of inertia, rigidity, or other mechanical properties. This ability is thought to depend on a central representation (internal model) of the dynamics of the interaction between the human subject and the manipulated object (Kawato 1999), which we will henceforth refer to as manipulation dynamics. In the context of this study, an internal dynamics model comprises neural mechanisms that represent the transformation from neural command to movement of a handheld object or the inverse transformation.

The cerebellum and primary motor cortex appear to be the regions of the brain most directly implicated in the formation and implementation of internal dynamics models. In particular, the ipsilateral cerebellum shows changes in regional cerebral blood flow during adaptation to novel manipulation dynamics that appear to be related to changes in motor error (Nezafat et al. 2001). Furthermore, individuals with cerebellar atrophy are less able to adapt to novel manipulation dynamics than control subjects (Maschke et al. 2004), and individuals with cerebellar lesions do not update motor commands based on past error (Smith and Shadmehr 2005) unlike control subjects. Other evidence from fMRI studies suggests that the cerebellum is involved in forming and implementing representations of novel transformations between hand and cursor motion (Imamizu et al. 2000, 2003). Evidence for involvement of primary motor cortex is based primarily on single unit recordings from non-human primates. Studies of changes in manipulation dynamics with non-human primates have reported shifts in the preferred directions of neurons in primary motor area (M1) (Li et al. 2001) and to a lesser extent in supplementary motor area (SMA) (Padoa-Schioppa et al. 2004) that develop during adaptation and are retained after washout. However, there are major outputs from the cerebellum to M1 and minor outputs to SMA (Sakai et al. 2002), so it is possible that underlying changes in cerebellar activity may be responsible for the observed changes in M1 and SMA.

In fact, there are reciprocal or recurrent pathways between the cerebellum and primary motor cortex (Holdefer et al. 2000; Middleton and Strick 2000) that appear to be functionally organized such that the regions in each structure that represent the same anatomical region are connected. The pathway from the cortex to the cerebellum is believed to provide the cerebellum with a copy of the motor command being sent to the muscles through the mossy fiber input (efference copy). The climbing fiber input to the cerebellum is thought to provide a training signal related to error, which leads to adaptive changes in the output of the cerebellum. There are several models for how this takes place. One that has received much attention is feedback error learning, which asserts that the climbing fibers provide a feedback error representing error in the motor command that is used to form an internal dynamics model by an iterative corrective process (Kawato 1990). However, this concept has recently been questioned on the grounds that climbing fibers are primarily activated by sensory inputs, so an alternative model of cerebellar adaptation has been proposed based on recurrent cerebellar connectivity (Porrill et al. 2004).

To test the hypothesis that cerebellar activity more closely represents implementation of an internal model than does activity in primary motor cortex, we designed an fMRI experiment in which subjects balanced similar objects that differed markedly in their dynamic behavior. We varied the complexity of the manipulation dynamics by altering the mechanical stability and the flexibility of the objects to vary the extent to

Address for reprint requests and other correspondence: T. E. Milner, School of Kinesiology, Simon Fraser University, Burnaby, B.C. V5A 1S6, Canada (E-mail: tmilner@sfu.ca).

The costs of publication of this article were defrayed in part by the payment of page charges. The article must therefore be hereby marked "*advertisement*" in accordance with 18 U.S.C. Section 1734 solely to indicate this fact.

which an internal model of the manipulation dynamics was required in the moment-to-moment control of the object's orientation. We compared manipulation of the same object in a stable state and a highly unstable state as well as comparing manipulation of a rigid object and a flexible object in the same unstable state. From earlier studies, we expected that activity in both primary motor cortex and cerebellum, relative to resting baseline, would increase in proportion to muscle activation (Dai et al. 2001; Dettmers et al. 1996; Ehrsson et al. 2001; Kuhtz-Buschbeck et al. 2001; Thickbroom et al. 1998). However, we predicted that for similar levels of muscle activation we would find little or no difference in primary motor cortex activity but marked differences in activation of the cerebellum because of its involvement in internal model-based control. We conducted whole-brain fMRI to test this prediction. Although we were not able to match the level of muscle activation across conditions, we did find dramatic differences in cerebellar activation that appeared to be more closely linked to manipulation dynamics than muscle activation.

METHODS

Subjects and general procedure

Nineteen neurologically normal subjects participated in the fMRI experiment. Nine of these subjects and three additional subjects participated in a second psychophysical experiment. Five of these subjects and six additional subjects participated in a third experiment to estimate grip force. All subjects gave informed consent to the procedures that were approved by the institutional ethics board and conformed to the Declaration of Helsinki. Subjects performed an object manipulation task while lying in the supine position. All subjects performed the task with the right hand. The conditions consisted of holding a flexible object in a stable equilibrium position (stable), balancing a rigid object at an unstable equilibrium position (unstable·r), balancing the flexible object at an unstable equilibrium position (unstable·f) and relaxing (rest). The condition changed every 30 s.

Protocol

In the fMRI experiment, there was a 6-s interval between conditions during which the experimenter prepared the subject for the next condition. The subject went through the conditions five times in one order and then five times in the reverse order. The condition order was varied randomly among subjects. The experimenter stood at the subject's side throughout the recording session and placed the object in the subject's hand prior to the start of each 30-s scan. At the end of the scan, the current object was removed from the subject's hand and reoriented or replaced according to the condition order.

Because of the position of the subject's head in the gantry of the scanner, the subject could not see the objects. Therefore the task was performed using only somatosensory feedback. When holding an object, subjects rested their forearm on a soft support surface, although the wrist remained unsupported. The flexible object consisted of a thin plastic ruler with two 130-g weights centered 25 cm from the center of the grip position (Fig. 1). The rigid object was a rectangular piece of wood of the same length and width as the plastic ruler, but considerably thicker, with identical weights positioned at the same distance from the center of the grip position. Thin wooden blocks were attached to either side of the plastic ruler with double-sided tape to serve as grip surfaces. The blocks allowed texture, friction, and thickness of the grip surfaces to be matched across conditions. When either object was gripped below the weight, it was in a mechanically unstable state. When the ruler was inverted with the weight below the hand, it was in a mechanically stable state. Subjects held the object in a pinch grip between the thumb and two or three fingers. They were instructed to maintain the weight directly above the hand under the unstable conditions, i.e., not to allow it to deviate from vertical. Their task under the stable condition was to hold the flexible ruler with a grip force that they perceived as matching their grip force under the unstable condition. We wish to emphasize that although the difficulty varied greatly between controlling the orientation under the stable versus the unstable conditions, extensive training was not required to perform the task successfully. All subjects were given sufficient practice with each condition prior to the experiment to master the control of each object. Furthermore, the majority of the subjects had previously participated in an experiment, which involved controlling the orientation of the flexible object under identical conditions.

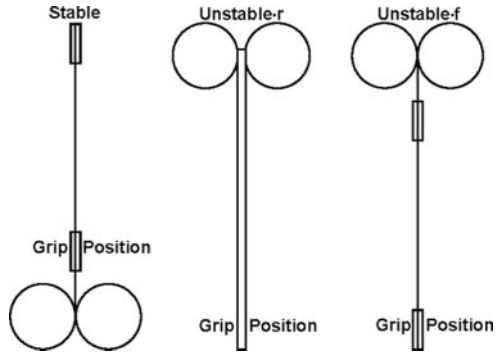

FIG. 1. Objects are shown in the orientation in which subjects were instructed to hold them. The grip position on each object is indicated. The objects under the stable and unstable·f conditions differed only in orientation.

Psychophysical experiment

For eight subjects, the motion of the object being held was tracked using an OPTOTRAK system (Northern Digital) while they performed the task in the MRI scanner. Infrared light emitting diodes (IREDs) were mounted at the center of each grip surface and at the center of the weight on each object. We discovered later that activation of the IREDs introduced noise into the MRI signal. Consequently, we had these subjects repeat the experiment a second time without motion tracking, although the original OPTOTRAK recordings were included in the analysis described in the following text.

In the psychophysical experiment, 12 subjects performed four repetitions of the four conditions outside of the scanner. The condition order was randomized and also performed in the reverse order as in the scanner. Subjects reclined on a mat, adopting the same body posture as during the brain imaging. Their right arm was similarly supported, and subjects again received no vision of their hand or the object while performing the task. As well as tracking the motion of the object with the OPTOTRAK system at 300 Hz, EMG was recorded with surface electrodes placed over the flexor pollicis brevis, first dorsal interosseus, biceps brachii, flexor carpi radialis, pronator teres, extensor carpi ulnaris, and extensor carpi radialis longus muscles of the right hand. Because flexor pollicis brevis is relatively small, the electrode overlying the muscle may have also picked up activity from the adductor pollicis muscle. The EMG was recorded using a Delsys Bagnoli 16 system, which amplified and band-pass filtered the signals between 20 Hz (high-pass) and 450 Hz (low-pass). EMG signals were then sampled at 2 kHz and stored for later analysis. Torque about the center of the grip position was computed from the position of the center of the weight relative to the center of the grip position. The absolute value of the torque was integrated over time and its mean value and variance were computed for comparison across conditions using repeated-measures ANOVA. Because the center of the weight was at a fixed distance from the center of the grip position for the two

unstable objects, mean torque is equivalent to average inclination of the object relative to vertical, whereas torque variance is equivalent to position variance of the center of the weight. The root mean square (rms) EMG for each muscle was also computed for comparison across conditions. After subtracting the rms EMG of the relaxed state (rest condition), statistical comparisons were made using repeated-measures ANOVA. Significant effects were then examined using Scheffe's post hoc test to look at differences across conditions.

Grip force experiment

A miniature load cell (LM-2KA-P, Kyowa) sandwiched between two thin wooden surfaces was used to measure the maximum grip force of 11 subjects. The load cell apparatus was then attached in place of one of the grip surfaces on each object, and the subject performed the same manipulation task as in the fMRI experiment, under the three stability conditions. Grip force was first recorded for three maximal efforts. The subject then performed the manipulation task under each condition for 30 s and the mean grip force over the last 20 s was computed. Each condition was repeated twice. The mean grip force for each condition was expressed as a percentage of the subject's maximum grip force.

Brain imaging

The 1.5 T MRI scanner (Shimadzu-Marconi) in the ATR Brain Activity Imaging Center was used to obtain blood-oxygenation-level-dependent (BOLD) contrast functional images. High-resolution anatomical (structural) images were obtained with a T_1-weighted sequence for each subject. Functional images weighted with the apparent transverse relaxation time (T_2*) were obtained with an echo-planar imaging sequence (repetition time = 5.4 s, echo time = 65 ms, flip angle = 90°). 92 sequential whole brain volumes (64 × 64 × 50 voxels at 3 mm isotropic resolution) were acquired in each session.

We used SPM 99 software (http://www.fil.ion.ucl.ac.uk/spm/) to analyze the images. The first two image volumes were discarded to allow for T_1 equilibration. The remaining 90 image volumes were realigned to the first volume and normalized to the Montreal Neurological Institute (MNI; Montreal, Canada) reference brain. The data were spatially smoothed with a Gaussian kernel with 6-mm full width at half-maximum (FWHM). The voxel time series were temporally smoothed with a Gaussian filter (FWHM of 4 s). Anatomical regions were identified from normalized T1 structural images averaged across subjects, using the Automated Anatomical Labeling method of Tzourio-Mazoyer et al. (2002), and functional anatomy was determined from the Brodmann map as implemented in the FWU pick atlas (Maldjian et al. 2003, 2004).

Statistical analysis

Statistical parametric maps of *t*-statistics were calculated for condition specific effects (stable, unstable·r, unstable·f, and rest) within a general linear model. We computed the statistical images corresponding to the contrasts: (unstable·f-stable), (unstable·r-stable), (unstable·f-unstable·r) and each manipulation task minus the resting baseline (level 1). The contrast images obtained from level 1 were entered into a second level *t*-test to create an SPM {*t*} map and were analyzed using a random effects model to accommodate intersubject variability in group analysis (Penny and Holmes 2003; Schmitz et al. 2005). A one-sample *t*-test was used (18 df). Voxels were identified at $P < 0.05$ after correction for multiple comparisons. The condition specific effects were first tested for significance for every voxel from the brain. Linear contrasts between conditions were used to create activation maps. From these activation maps we determined the locations of local maxima of activity for which $t(18) > 7.64$ ($P < 0.05$ when corrected for multiple comparisons for the whole brain volume). Region of interest (ROI) masks were created for the anatomical regions in which the local maxima were located. Further analysis was restricted to these ROIs to increase sensitivity. Three ROIs were identified, namely the ipsilateral cerebellar hemisphere, contralateral M1 (Brodmann area 4) and a region in the ipsilateral inferior parietal lobule that included the postcentral gyrus, inferior parietal gyri and superior parietal gyrus. The random effects analysis was then repeated with the correction for multiple comparisons restricted to the smaller volume of the ROIs (Worsely et al. 1996). Figure 2 shows the three-dimensional projections of these ROIs onto the sagittal, coronal and transverse planes.

Because the degree of difficulty in performing the task varied considerably between the stable and unstable conditions, we wanted to ensure that the amount of head movement did not vary with the stability of the object. We estimated the amount of head movement from post hoc

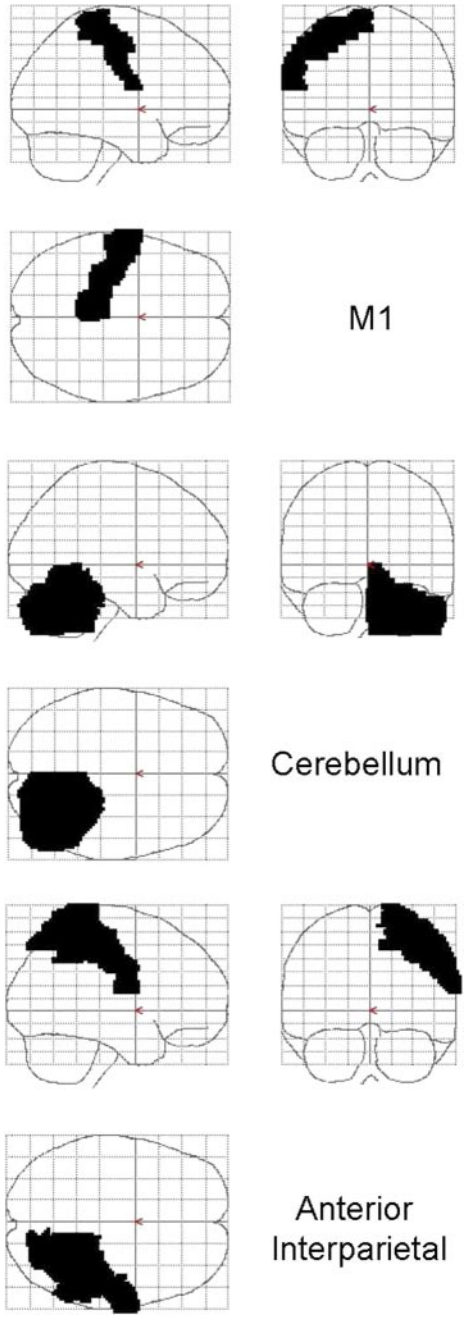

FIG. 2. Planar projections of the 3 region of interest (ROI) masks The red arrows indicate the location of the origin of the Montreal Neurological Institute (MNI) coordinate system.

TABLE 1. *Manipulation tasks versus baseline*

Anatomical Region	MNI Coordinates			Peak z Score	Cluster Size†*	P Value†
	x	y	z			
Stable versus baseline						
Left primary motor cortex (M1)	−48	−14	56	4.42	4‡	0.013
Unstable-r versus baseline						
Left primary motor cortex (M1)	−36	−18	50	5.02	194‡	0.001
Right cerebellum (lobule V/VI lateral)	22	−50	−26	5.35	89	0.001
Right cerebellum (lobule V/VI medial)	4	−66	−14	4.65	6	0.018
Unstable-f versus baseline						
Left primary motor cortex (M1)	−38	−18	52	5.68	350	<0.001
Right cerebellum (lobule V/VI lateral)	16	−52	−22	5.59	244	<0.001
Right cerebellum (lobule V/VI medial)	4	−68	−16	4.87	13	0.007
Right cerebellum (lobule VIIIB/IX)	14	−64	−50	4.64	7	0.019

*Number of 8 mm^3 voxels in cluster, †Corrected P values using a small volume correction, ‡Cluster was not contiguous.

realignment of MR images and compared the maximum absolute difference in head position and orientation for rest, stable, unstable·r, and unstable·f conditions. The absolute difference in each coordinate was averaged across repetitions of the epoch for each subject. The averaged differences (19 subjects × 4 condition × 6 coordinates) were analyzed by a two-way (condition × coordinate) ANOVA. There was no significant effect of the condition [$F(3,432) = 1.55$, $P > 0.201$]. Furthermore, the mean of the maximum head displacement over the 30-s intervals did not exceed 0.1 mm in any direction.

RESULTS

Brain activation: all manipulation conditions minus rest

We identified three ROIs from the whole brain analysis (Fig. 2). These were the only regions in which a significance level of $P < 0.05$ (corrected for multiple comparisons) was reached in any of the contrasts. Using the ROI masks, we then located the local maxima of voxel clusters. The anatomical locations of these maxima are listed in Table 1. The contrasts with respect to the resting baseline revealed several important features of the task-related brain activation. First, there was a relatively large region near the border of the anterior and superior posterior lobes of the ipsilateral cerebellum, lateral to the midline, and a much smaller region closer to the midline where activity was statistically significant under both unstable conditions. In contrast, there was no statistically significant activity anywhere in the cerebellum under the stable condition. Second, there was a small focus of activation in the ipsilateral biventer lobule under the unstable·f condition. Third, the total activated volume of the contralateral M1 was almost two orders of magnitude greater under either unstable condition than under the stable condition. Finally, activity in the ipsilateral inferior parietal lobule was not statistically significant for any of the conditions relative to the resting baseline.

Table 2 compares the number of activated voxels in contralateral M1 and ipsilateral cerebellum for $P < 0.001$ (uncorrected). These results are included for comparison with the studies of Thickbroom et al. (1998) and Dai et al. (2001) to assess whether changes in activation of M1 and cerebellum with the stability condition might simply be related to changes in grip force or muscle activation.

Brain activation: stability contrasts

The principal objective of this study was to compare activation in M1 and cerebellum for (unstable·f-stable), (unstable·r-stable), and (unstable·f-unstable·r) contrasts. For completeness, we also examined the reverse contrasts, but these showed no statistically significant activity anywhere in the brain. For the unstable·f-stable contrast, we found that a small region in the contralateral M1 and a much larger region near the border of the anterior and superior posterior lobes of the ipsilateral cerebellum were activated as well as a small region near the anterior edge of the ipsilateral inferior parietal lobule (Fig. 3). The regions in M1 and cerebellum were located in areas previously shown to be activated during finger, hand, and elbow movements (Grodd et al. 2001; Kawashima et al. 1995). Of particular interest, is that the region in the cerebellum had two foci, separated by ~12 mm (Fig. 3). When we contrasted unstable·r-stable, we found that the only activated region was in M1 and that it comprised a small fraction (~8%) of the activated region identified in the unstable·f-stable contrast. On the other hand, for the unstable·f–unstable·r contrast there was no significant activation in M1, but a significant portion of the cerebellar region identified in the unstable·f–stable contrast was activated (~30%). However, there was only one focus of activation in the cerebellum that was ~4.5 mm from the more lateral focus of activation in the unstable·f-stable contrast. There was again a focus of activation in the ipsilateral inferior parietal lobule which was shifted ~14 mm inferior to that of the unstable·f-stable contrast. The anatomical locations of all maxima are listed in Table 3.

Psychophysical results

To confirm that learning did not play a part in the observed differences in BOLD signals, we compared the mean torque

TABLE 2. *Comparison of number of activated voxels in M1 and cerebellum*

Anatomical Region	Number of Voxels	*P* Value*
Stable versus baseline		
Left primary motor cortex (M1)	162	0.001
Right cerebellum	24	0.001
Unstable-r versus baseline		
Left primary motor cortex (M1)	696	0.001
Right cerebellum	652	0.001
Unstable-f versus baseline		
Left primary motor cortex (M1)	851	0.001
Right cerebellum	1057	0.001

*Not corrected for multiple comparisons as in Thickbroom et al. (1998).

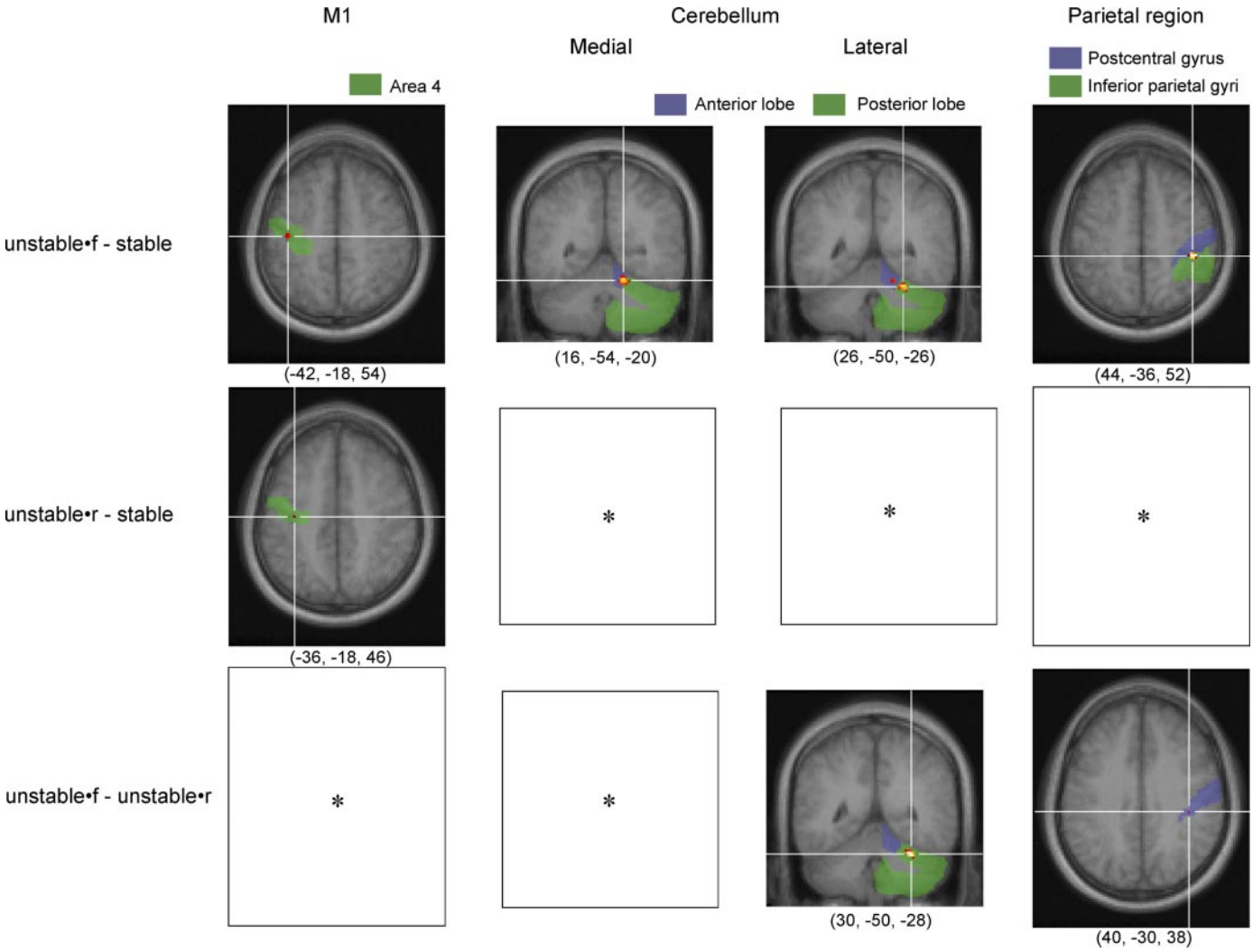

FIG. 3. ROI masks (blue and green regions) and foci of activity for the unstable·f-stable contrast (*top*), the unstable·r-stable contrast (*middle*), and the unstable·f-unstable·r contrast (*bottom*). Asterisks (*) indicate that there was no significant activation in the corresponding region. Anatomical images were normalized and averaged across subjects. Transverse slices corresponding to locations of local maxima are shown for M1 and inferior parietal lobule; coronal slices are shown for cerebellum. Coordinates of local maxima shown below each slice correspond to those listed in Table 3.

and torque variance between the first and last two 30-s blocks in the case of the unstable conditions for the eight subjects for whom we had OPTOTRAK data in the MRI scanner. Note that these measures are equivalent to the average inclination and the position variance of the object, respectively. We found no significant difference in either the absolute torque ($P = 0.41$ for unstable·r, $P = 0.31$ for unstable·f) or the torque variance ($P = 0.34$ for unstable·r, $P = 0.66$ for unstable·f). Thus subjects' performance, as represented by their ability to maintain the object in a vertical position or by the amount that the

TABLE 3. *Task specific activations*

Anatomical Region	MNI Coordinates			Peak z Score	Cluster Size*	P Value†
	x	y	z			
Unstable-r versus stable						
Left primary motor cortex (M1)	−36	−18	46	4.08	1	0.038
Unstable-f versus stable						
Left primary motor cortex (M1)	−42	−18	54	4.21	12	0.024
Right cerebellum (lobule V/VI lateral)	26	−50	−26	4.82	80	0.009
	16	−54	−20	4.74		0.013
Right inferior parietal lobule	44	−36	52	5.95	19	<0.001
Unstable-f versus unstable-r						
Right cerebellum (lobule V/VI lateral)	30	−50	−28	5.46	25	<0.001
Right inferior parietal lobule	40	−30	38	4.21	1	0.048

*Number of 8 mm^3 voxels in cluster, †corrected P values using a small volume correction.

object moved, did not change significantly over the course of the experiment, providing evidence that learning did not occur.

There was no significant difference in the mean absolute torque between the two unstable conditions (Fig. 4A). However, the mean absolute torque was lower under the stable condition ($P < 0.05$). Note that because subjects did not maintain the object in an orientation that was exactly vertical or perfectly stationary, the mean absolute torque was not zero, even under the stable condition. The torque variance was higher under the unstable·f condition than under the stable or unstable·r conditions, suggesting that flexibility made the object more difficult to control. This was also confirmed from analysis of the object movement for the eight subjects noted in the preceding text. We computed an average magnitude for the angular velocity of the object from the variation in the orientation of the object, which was 0.058 ± 0.017 (SD) rad/s under the unstable·f condition compared with 0.023 ± 0.012 rad/s under the unstable·r condition and 0.022 ± 0.018 rad/s under the stable condition. The angular velocity was quite small under all conditions, i.e., movement of the hand was generally not noticeable. However, although there was no difference in the movement of the object under the unstable·r and stable conditions ($P = 0.89$), there was significantly more movement under the unstable·f condition than either the unstable·r ($P < 0.0001$) or stable condition ($P = 0.0012$).

There was no difference in the rms EMG of the more proximally acting muscles (prontator teres and biceps brachii) between conditions. However, there were significant differences for wrist and finger muscles (Fig. 4*B*). In the case of the wrist, the rms EMG of the wrist flexor (flexor carpi radialis) and extensor muscles (extensor carpi radialis longus and extensor carpi ulnaris) under the unstable·f condition was significantly higher than under the stable condition ($P < 0.05$), indicating that wrist stiffness was increased by muscle cocontraction. Wrist stiffness was likely also higher under the unstable·f condition than under the unstable·r condition since the rms EMG of the wrist extensor muscles was significantly higher ($P < 0.05$). In the case of the finger muscles, the rms EMG of flexor pollicis brevis was significantly higher under the unstable·f condition than under the unstable·r condition and it was significantly higher under both unstable conditions than under the stable condition ($P < 0.05$). The rms EMG of first dorsal interosseus was significantly higher under the unstable conditions than the stable condition ($P < 0.05$). This would suggest that the grip force was lowest in the stable condition, higher in the unstable · r condition, and highest in the unstable·f condition. However, the grip force experiment suggested that there was relatively little difference among stability conditions. The mean values across subjects ranged from ~10% of maximum grip force for the stable and unstable·r condition to 12% for the unstable·f condition, although these differences were not statistically significant ($P > 0.28$).

The variation in muscle activation with the stability of the manipulation dynamics introduced a potential confounding factor that we will consider now. Three previous studies were specifically designed to examine how the fMRI signal varies with hand force and muscle activation. The first of these (Dettmers et al. 1996) focused on a single slice through M1 and posterior supplementary area and found that signal intensity increased in a logarithmic fashion for index finger forces between ~5 and 40% of maximum force. The second study (Thickbroom et al. 1998) examined the entire contralateral primary sensorimotor cortex and found that there was a relatively greater increase in voxel number than mean signal per voxel for finger flexion forces between 5 and 50% of maximum. The third study (Dai et al. 2001) examined multiple motor-related areas of the brain in a power grip task, but over a different force range (20–80% of maximum). The ROIs included those relevant to our study, namely contralateral M1 and cerebellum, although the entire cerebellum was treated as one region of interest. They showed that both the average intensity and the number of activated pixels increased in a linear or less than linear fashion with grip force and with rectified averaged surface EMG of the long finger flexor and extensor muscles. All of these studies suggest that the number of activated voxels should increase monotonically but not more than linearly with grip force or EMG if the activation of a region simply reflects the amount of muscle activation needed to perform the task.

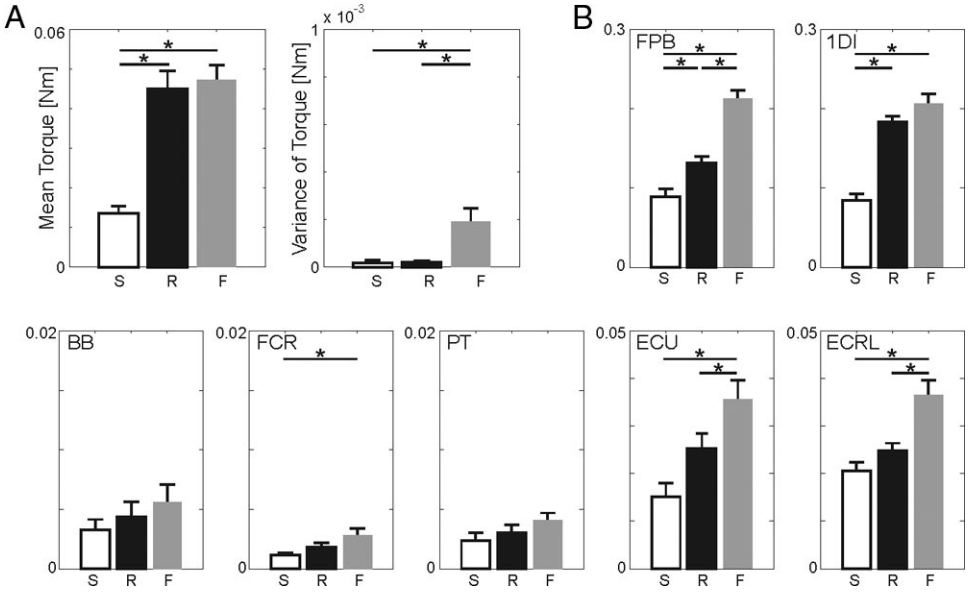

FIG. 4. *A*: mean torque and torque variance under stable (S), unstable·r (R), and unstable·f (F) conditions with SEs ($n = 16$). *B*: mean root mean square (rms) EMG with standard errors ($n = 12$) for flexor pollicis brevis (FPB), 1st dorsal interosseus (1DI), biceps brachii (BB), flexor carpi radialis (FCR), pronator teres (PT), extensor carpi ulnaris (ECU), and extensor carpi radialis longus (ECRL) muscles. *, statistically significant differences ($P < 0.05$).

Because grip force did not vary by >20% across stability conditions based on our estimates, changes in grip force could not account for changes in activation of any of the activated brain structures. Activity of hand and wrist muscles, however, increased by as much as 200–300% between the stable and unstable·f conditions (Fig. 4). A 300% increase in muscle activation could account for at least half the increase in activated voxels in M1 between the stable and unstable·f conditions assuming a linear relation between EMG and voxel number (Table 2). On the other hand, it would not account for >7% of the increase in activated voxels in the cerebellum. There was a much smaller increase in the number of activated voxels in both M1 and cerebellum between unstable·r and unstable·f conditions, similar to the difference in muscle activation between the two conditions.

DISCUSSION

As we hypothesized, when the brain activity under the stable condition was subtracted from that under the unstable conditions, it became evident that the dynamics-related activation of the cerebellum was quite different from that of the primary motor cortex. In the discussion that follows, we propose that cerebellar activity was indicative of moment-to-moment predictive control derived from an internal dynamics model, whereas the activity of the primary motor cortex more closely resembled the mean motor output necessary to execute the task. Somewhat unexpectedly, we found an ipsilateral region near the anterior edge of the inferior parietal lobule where activity was also modulated with the stability of the manipulation dynamics. This region appears to be important in complex hand manipulation.

Condition-dependent differences in muscle activation

The experiment was designed to match muscle activity under the unstable and stable conditions by instructing subjects to exert excessive grip force in the stable condition. However, the EMG records clearly indicate that despite this explicit instruction, muscle activation was modulated with the stability of the manipulation dynamics. Torque was required to move the weight to the upright position whenever it deviated or to maintain the weight at a deviated position when the subject failed to perceive that it had drifted from upright. The object was moved principally by "rolling" action of the thumb and fingers. Consequently the activity of thumb and finger muscles served both to grip and apply torque to the object. To keep the wrist stationary, the activity of wrist muscles had to be modulated to balance torque arising from thumb and finger muscles crossing the wrist and to increase joint stiffness for stability. The variation in the rms EMG of finger and wrist muscles with the stability of the manipulation dynamics can be explained by the differences in the mean absolute torque and the torque variance, which created demands for muscle activation in addition to those required for grip force. Thus mean grip force may have been the same across stability conditions, but muscle activation increased as stability decreased and control became more complex.

Previous fMRI studies of manipulation

Ehrsson et al. (2001, 2003) and Kuhtz-Buschbeck et al. (2001) identified a number of regions in frontal and parietal cortex that were activated in relation to different aspects of manipulation with precision grip. The study by Kuhtz-Buschbeck et al. (2001) was the most similar to our study in that subjects continuously maintained the same grip force for ~40 s, although grip initiation, lifting of the object, setting the object down, and releasing the grip were also part of the task. When subjects used a firm grip, the contralateral primary sensorimotor areas, premotor areas (PMd and PMv) and Brodmann area 7 were activated along with Brodmann area 40 bilaterally. The cerebellum, however, was outside the field of view. The principal difference with our study is that we did not find significant activation of contralateral premotor areas or contralateral areas 7 and 40. The main reason for this may be that their task would have involved decision and planning phases for initiating and releasing the grip, which were absent in our task.

Activity in cerebellum and primary motor cortex

Based on the analysis of number of activated voxels in Table 2, it appears that activity in the cerebellum represents the stability of the manipulation dynamics, although it does not provide a clear indication that complexity of the manipulation dynamics (unstable·f vs. unstable·r) is independently represented. The stability contrasts (Table 3), on the other hand, suggest that both stability and complexity of the dynamics are represented in the cerebellum as opposed to M1. The differences in activation of contralateral M1 seen in the stability contrasts were similar to the differences in mean absolute torque but not to the differences in torque variance under the three stability conditions. The case was reversed for the ipsilateral cerebellum. We found no significant difference in the mean absolute torque between the two unstable conditions, whereas it was significantly less under the stable condition than under either of the unstable conditions. Correspondingly, we found no significant activation of contralateral M1 for the unstable·f–unstable·r contrast and significant activation for both the unstable·f–stable and unstable·r–stable contrasts. This would suggest that changes in activation of M1 with the manipulation dynamics primarily reflect changes in mean levels of muscle activation.

In the case of the torque variance, we found no significant difference under the stable and unstable·r conditions but a marked increase under the unstable·f condition relative to the other two conditions. This corresponds with the finding that there was no significant activation of the ipsilateral cerebellum for the unstable·r-stable contrast and significant activation for both the unstable·f–stable and unstable·f–unstable·r contrasts. The torque variance reflects changes in torque over time required to correct for deviation of the object from a vertical orientation. Therefore it can be thought of as a measure of the moment-to-moment changes in muscle activation needed to control the orientation of the object. The cerebellum has been implicated in both feedback and feedforward control of movement. In the one case, it regulates feedback gains (MacKay and Murphy 1979) and in the other it represents the system dynamics (Nezafat et al. 2001). That there was no activation of the cerebellum under the stable condition compared with the resting baseline could be interpreted as indicating that in the stable state the object is balanced with little feedback regulation and without the need for representation of the manipulation dynam-

ics. The constant control signal needed to activate the appropriate muscles would have required little of the cerebellum's capacity for neural computation.

In contrast, feedback control and/or predictive feedforward control was essential under the unstable conditions. The type of afferent information available for control should have been the same under all conditions, according to the experimental design, although there would have been little need to process the afferent information under the stable condition. Greater cerebellar activation under the unstable·f than the unstable·r condition could be interpreted in two ways. It is possible that it simply reflects the greater muscle activation employed under the unstable·f condition. On the other hand, the identification of two foci of activation in the unstable·f-stable contrast, one of which disappeared in the unstable·f-unstable·r contrast, could also reflect the need for activation of a larger neural network to represent the more complex manipulation dynamics of the flexible object, which was more difficult to control as indicated by the greater torque variance. Overall, our results are consistent with the view that considerably more computational resources were devoted to the transformation of afferent input to motor output under the unstable conditions than under the stable condition.

Cerebellum and internal models

Imamizu et al. (2000) found a region of the cerebellum that was selectively activated when subjects were required to make a visuomotor transformation to track a moving target. The region was bilateral and extended toward the lateral boundaries of the cerebellum. They later showed that different regions were activated when the visuomotor transformations were different, although there was some overlap (Imamizu et al. 2003). They interpreted their results in terms of separate internal representations or models for different transformations. Kawato et al. (2003) argued that the contralateral cerebellum was the site of such an internal model for the coordination of grip force with load force during object transport, although they did identify another candidate region in the ipsilateral cerebellum close to the activated regions under the unstable·r and unstable·f conditions of our study. It is possible that a portion of the activated region under the unstable·r condition represents implementation of an internal model of the manipulation dynamics of a rigid inverted pendulum and that the expansion of this region or the appearance of a second focus of activation under the unstable·f condition represents the added complexity of manipulating an inverted pendulum with a flexible shaft.

Inferior parietal lobule

The activated region that we identified near the anterior edge of the ipsilateral inferior parietal lobule showed statistically significant activation under the unstable·f condition relative to the two other conditions but not relative to the resting baseline. Because it was not activated under the unstable·r condition relative to the stable condition, its activity would appear to be related principally to the complexity of the manipulation rather than to its stability. Bilateral activation of this general region of the brain has been linked to three-dimensional object features that are related to aspects of visually guided grasping, such as hand shape, aperture, or orientation (Binkofski et al. 1999). However, this region has also been shown to be activated bilaterally during exploration of complex shapes in the absence of vision (Jäncke et al. 2001). In these previous studies, this region was referred to as the anterior intraparietal area (AIP), although it is not clear yet whether it is analogous to AIP in the monkey. The most surprising finding in our study was that it was activated only on the ipsilateral (right) side, although this would be consistent with the spatial function of the right hemisphere because our task was purely spatial. The need to involve parietal cortex was likely related to imagining the position and motion of the flexible ruler while controlling it without vision. Because the exploration task of Jäncke et al. (2001) also had a verbal component, i.e., subjects manipulated shapes that could be named (hammer, bag, cup, umbrella, car) and the purpose of the manipulation was to identify the shapes, subjects in their study also activated the left hemisphere.

In summary, our results indicate that the cerebellum is differentially activated for manipulation of an object that is mechanically unstable compared with one that is mechanically stable. In addition, cerebellar activation appears to discriminate features of the manipulation dynamics that are not represented in M1. We, therefore propose that the cerebellar activity represents the implementation of an internal dynamics model of the object manipulation that is necessary for feedback control. We also found differential activation of a region near the anterior edge of the inferior parietal lobule of the right hemisphere in relation to the complexity of the manipulation dynamics. This is likely related to having to imagine the location and motion of an object with complex manipulation dynamics when controlling it without vision.

ACKNOWLEDGMENTS

We thank G. Liaw for assisting in the second experiment.

GRANTS

This work was supported by National Institute of Information and Communications Technology and National Sciences and Engineering Research Council.

REFERENCES

Binkofski F, Buccino G, Posse S, Seitz RJ, Rizzolatti G, and Freund H. A fronto-parietal circuit for object manipulation in man: evidence from an fMRI-study. *Eur J Neurosci* 11: 3276–3286, 1999.

Dai TH, Liu JZ, Sahgal V, Brown RW, and Yue GH. Relationship between muscle output and functional MRI-measured brain activation. *Exp Brain Res* 140: 290–300, 2001.

Dettmers C, Connelly A, Stephan KM, Turner R, Friston KJ, Frackowiak RS, and Gadian DG. Quantitative comparison of functional magnetic resonance imaging with positron emission tomography using a force-related paradigm. *Neuroimage* 4: 201–209, 1996.

Ehrsson HH, Fagergren A, and Forssberg H. Differential fronto-parietal activation depending on force used in a precision grip task: an fMRI study. *J Neurophysiol* 85: 2613–2623, 2001.

Ehrsson HH, Fagergren A, Johansson RS, and Forssberg H. Evidence for the involvement of the posterior parietal cortex in coordination of fingertip forces for grasp stability in manipulation. *J Neurophysiol* 90: 2978–2986, 2003.

Grodd W, Hülsmann E, Lotze M, Wildgruber D, and Erb M. Sensorimotor mapping of the human cerebellum: fMRI evidence of somatotopic organization. *Hum Brain Map* 13: 55–73, 2001.

Holdefer RN, Miller LE, Chen LL, and Houk JC. Functional connectivity between cerebellum and primary motor cortex in the awake monkey. *J Neurophysiol* 84: 585–590, 2000.

Imamizu H, Kuroda T, Miyauchi S, Yoshioka T, and Kawato M. Modular organization of internal models of tools in the human cerebellum. *Proc Natl Acad Sci USA* 100: 5461–5466, 2003.

Imamizu H, Miyauchi S, Tamada T, Sasaki Y, Takino R, Putz B, Yoshioka T, and Kawato M. Human cerebellar activity reflecting an acquired internal model of a new tool. *Nature* 403: 192–195, 2000.

Jäncke L, Kleinschmidt A, Mirzazade S, Shah NJ, and Freund H-J. The role of the inferior parietal cortex in linking the tactile perception and manual construction of object shapes. *Cereb Cortex* 11: 114–121, 2001.

Kawashima R, Itoh H, Ono S, Satoh K, Furumoto S, Gotoh R, Koyama M, Yoshioka S, Takahashi T, Yanagisawa T, and Fukuda H. Activity in the human primary motor cortex related to arm and finger movements. *Neuroreport* 6: 238–240, 1995.

Kawato M. Feedback-error-learning neural network for supervised motor learning. In: *Advanced Neural Computers,* edited by Eckmiller R. Amsterdam: Elsevier, 1990, p. 365–372.

Kawato M. Internal models for motor control and trajectory planning. *Curr Opin Neurobiol* 9: 718–727, 1999.

Kawato M, Kuroda T, Imamizu H, Nakano E, Miyauchi S, and Yoshioka T. Internal forward models in the cerebellum: fMRI study on grip force and load force coupling. *Prog Brain Res* 142: 171–188, 2003.

Kuhtz-Buschbeck JP, Ehrsson HH, and Forssberg H. Human brain activity in the control of fine static precision grip forces: an fMRI study. *Eur J Neurosci* 14: 382–390, 2001.

Li CS, Padoa-Schioppa C, and Bizzi E. Neuronal correlates of motor performance and motor learning in the primary motor cortex of monkeys adapting to an external force field. *Neuron* 30: 593–607, 2001.

MacKay WA and Murphy JT. Cerebellar modulation of reflex gain. *Prog Neurobiol* 13: 361–417, 1979.

Maldjian JA, Laurienti PJ, and Burdette JB. Precentral gyrus discrepancy in electronic versions of the Talairach atlas. *Neuroimage* 21: 450–455, 2004.

Maldjian JA, Laurienti PJ, Burdette JB, and Kraft RA. An automated method for neuroanatomic and cytoarchitectonic atlas-based interrogation of fMRI data sets. *Neuroimage* 19: 1233–1239, 2003.

Maschke M, Gomez CM, Ebner TJ, and Konczak J. Hereditary cerebellar ataxia progressively impairs force adaptation during goal-directed arm movements. *J Neurophysiol* 91: 230–238, 2004.

Middleton FA and Strick PA. Basal ganglia and cerebellar loops: motor and cognitive circuits. *Brain Res Rev* 31: 236–250, 2000.

Nezafat R, Shadmehr R, and Holcolmb HH. Long-term adaptation to dynamics of reaching movements: a PET study. *Exp Brain Res.* 140: 66–76, 2001.

Padoa-Schioppa C, Li CS, and Bizzi E. Neuronal activity in the supplementary motor area of monkeys adapting to a new dynamic environment. *J Neurophysiol 2004* 91: 449–473, 2004.

Penny WD and Holmes AJ. Random-effect analysis. In: *Human Brain Function* (2nd ed.), edited by Frackowiak RSJ, Friston KJ, Frith C, Dolan R, Price CJ, Zeki S, Ashburner J, and Penny WD, London: Academic, 2003, p. 843–850.

Porrill J, Dean P, and Stone JV. Recurrent cerebellar architecture solves the motor-error problem. *Proc R Soc Lond B Biol Sci* 271: 789–796, 2004.

Sakai ST, Inase M, and Tanji J. The relationship between MI and SMA afferents and cerebellar and pallidal efferents in the macaque monkey. *Somatosens Mot Res* 19: 139–148, 2002.

Schmitz C, Jenmalm P, Ehrsson HH, and Forssberg H. Brain activity during predictable and unpredictable weight changes when lifting objects. *J Neurophysiol* 93: 1498–1509, 2005.

Smith MA and Shadmehr R. Intact ability to learn internal models of arm dynamics in Huntington's disease but not cerebellar degeneration. *J Neurophysiol* 93: 2809–2821, 2005.

Thickbroom GW, Phillips BA, Morris I, Byrnes ML, and Mastaglia FL. Isometric force-related activity in sensorimotor cortex measured with functional MRI. *Exp Brain Res* 1998 121: 59–64, 1998.

Tzourio-Mazoyer N, Landeau B, Papathanassiou D, Crivello F, Etard O, Delcroix N, Mazoyer B, and Joliet M. Automated anatomical labeling of activations in SPM using a macroscopic anatomical parcellation of the MNI-MRI single subject brain. *Neuroimage* 15: 273–289, 2002.

Worsley KJ, Marrett S, Neelin P, Vandal AC, Friston KJ, and Evans AC. A unified statistical approach for determining significant signals in images of cerebral activation. *Hum Brain Map* 4: 58–73, 1996.